Conversion of actinide nitrate surrogates into oxide using combustion synthesis process: A facile approach

Julien Monnier, Cyrielle Rey, S. Chandra Mohan, J. Causse, E. Welcomme, Xavier Deschanels

1   **Conversion of actinide nitrate surrogates into oxide using combustion synthesis process:**

2   **A facile approach**

3   Monnier J.[1], Rey C. [1*], Chandra Mohan S. [1], Causse J. [1], Welcomme E. [2], Deschanels X. [1*]

4

5   [1] Institut de Chimie Séparative de Marcoule (ICSM) CEA, CNRS, ENSCM, Univ Montpellier, Marcoule,

6   France

7   [2] Laboratoire d'études des Procédés de Conversion des Actinides – LPCA – CEA Marcoule, CEA ; Nuclear

8   Energy Division, Research Department on Mining and Fuel Recycling Processes Service –

9   DEN\MAR\DMRC\SMFA\LPCA – F30207 Bagnols-sur-Cèze, France

10

11   Corresponding authors :

12   cyrielle.rey@umonpellier.fr

13   xavier.deschanels@cea.fr

14

Abstract

16   In recent years, the focus of research in the conversion routes for the actinide nitrates into oxides for the generation

17   IV nuclear fuel cycle have attracted rapidly growing interest. One process is the self-sustained exothermic reaction

18   of Solution Combustion Synthesis (SCS) methodology. It was applied here to the reaction of an actinide surrogate

19    $Gd(NO_3)_3,6H_2O$ with glycine in air to produce $\sim 10^{-3}$ mol amounts of Gd_2O_3. The primary process parameters were

20   the Gd/glycine ratio and heating rate, which affected the ignition temperature of the precursor mixture. An

21   optimum ratio of one and a heating rate of 10 $K.min^{-1}$ resulted in nearly complete SCS conversion over the 483-

22   573 K temperature range and ultrafine gadolinia powders. The 100- to 500-fold swelling of the reactant mixture

23   plays a dynamic role in the reactivity of the system. Final products were characterized by X-Rays Diffraction

24   (XRD), surface area analysis, carbon content, and Scanning Electron Microscopy (SEM). The structural

25   characteristics of the final gadolinia phases have been interpreted by the adiabatic flame temperature calculation.

26

27

28

Keywords

30   Actinide conversion - Gadolinium nitrate - Glycine - Combustion synthesis

31

32

33

34

35

Introduction

The recycling of actinides, in particular uranium and plutonium, resulting from the treatment of spent nuclear fuel, is of great interest for the deployment of Generation IV reactors (GEN IV) [1-2]. This recycling process involves a step of conversion of the actinides obtained in the form of nitrate in solution into an oxide form or more precisely a solid solution of mixed oxides (MOX). The conversion path should facilitate the formation of homogeneously mixed oxide compounds, containing different amounts of Pu (GEN III / GEN IV transition), in a continuous process. The resulting powders of mixed oxides must be adapted to a subsequent shaping of the fuel without any grinding step or sieving of the powders, in order to reduce the generation of dust.

In this direction, new routes have been experimented for the effective conversion of nitrates of actinides into oxides. Among the various routes, Solution Combustion Synthesis (SCS) is a simple and convenient path. Moreover, this is a self-sustaining exothermic redox reaction process between an oxidant (metal nitrate) and a reducing agent (organic fuel) mixed in an aqueous solution at the molecular level [3-7]. Under the thermal treatment of aqueous precursor, a self-sustaining reaction will occur when it reaches the ignition temperature. During this thermal treatment, the water is evaporated which leads to the conversion of the aqueous mixture into a gel ($\sim$ 373 K), and then, the gel is allowed to pyrolysis at a temperature of about 573 K. These two-step processes generate a large amount of gas, which makes the final product in porous and finely dispersed form [8]. These peculiarities of the SCS reactions seem interesting as regards to the synthesis of the solid solution of nanoscale actinide oxides [9-17]. However, the various controlling processing parameters plays a vital role to obtain the good characteristics for the finished products, but it is not well documented. In addition, the mechanism involved in the SCS reaction is not fully understood. The mechanism of SCS reaction mainly depends on the techniques used for the conversion reaction. Two modes can be distinguished: volume combustion, also known as a thermal explosion, and self-propagating combustion mode [18-19]. In the first mode, the entire volume of the precursor is uniformly heated to the ignition temperature and the temperature increases to a maximum value. In the second case, the precursor is heated locally to trigger the exothermic reaction, which propagates automatically over the entire volume of the precursor in the form of a combustion front. In this, the maximum temperature reached is lower than that observed in "volume combustion" mode [18].

Several equilibria such as thermal, chemical and structural are involved in a SCS reaction, and it depends on the kinetics of the reactions. The kinetics of the reaction could be strongly influenced by the various processing parameters. It is well known that the heating/cooling rate affects the SCS reaction leading to metastable phases [17]. The heating rate can also act on the generation of the gaseous compounds produced during the process, which can induce swelling of the viscous gel obtained by the dehydration of the precursors and it indirectly results in a modification of the reactivity. The fuel to oxidizer molar ratio, also called richness (see SI-1 for definition of ϕ), is another parameter which can affect the kinetic and the thermodynamic of the SCS reaction. For example, the adiabatic temperature reached during the SCS reaction is dependent on this parameter, and consequently it changes the characteristic of the powders synthesized.

In this present study, we studied the specific parameters such as swelling of the gel, temperature rate that provide a new and unique information for the SCS process. The experiments were carried out with gadolinium nitrate and glycine. The oxidation-reduction rate might be important in the conversion of actinides. So, gadolinium has been

considered as a surrogate for trivalent actinides (Cm, Am). Syntheses were carried out in a tubular furnace to perform a homogeneous volume heating of the sample and to control the thermal treatment. To gain better insights, modifications in the controlling parameters (heating rate, richness) were applied in the combustion process. The precursor was characterized by infrared spectroscopy (IR), thermal analysis coupled with mass spectrometry (TG-MS), the final products were analysed by X-ray diffraction (XRD), elemental analyses, scanning electron microscopy (SEM) and nitrogen adsorption-desorption isotherms (BET).

Experimental procedure

Gadolinium (III) nitrate hexahydrate (purity: 99.9%), Glycine anhydrous (purity: 99.5%) was purchased from Sigma Aldrich. Gd/Glycine was prepared by dissolving under stirring 2.10^{-3} mole of gadolinium nitrate hexahydrate in 3 mL of purified water, and an appropriate quantity of glycine to obtain the targeted richness ϕ (0.3 $< \phi < 2.2$).

Syntheses were performed in a tubular furnace (Nabertherm, Controller P320) under static air atmosphere. The heat treatment consists of rapid heating, up to 393 K, followed by a temperature plateau (dwell time 15 minutes) to dehydrate it and to obtain a gel called "dried gel" containing a mass of about 65-490 mg of Glycine and 550 mg of gadolinium nitrate. The resulting gel is then heated to 573 K with a variable heating rate (1 - 10 K.min^{-1}). The ignition of the SCS reaction was observed visually for a temperature in the range of 458 K and 513 K depending on the mixture chemical composition. After this treatment, a white powder was obtained.

IR spectra were recorded by using a spectrometer (Perkin-Elmer IR-ATR, spectrum 100) with a typical resolution of 8 cm^{-1} in the range of 300-1800 cm^{-1}. The Gd/Glycine gel was analysed after dehydration of the solution on a hot plate at 398 K and powders obtained after syntheses on tubular furnace were pressed on the lens thanks to a poppet.

The volume increase of the gel was measured in operando by direct observation of a graduated test tube (volume equal to 25 mL or 50 mL) put in the furnace. The initial volume of the dried gel is about 3 ml. A thermometer put on the test tube checked the temperature of the mixture.

ThermoGravimetric and Differential Thermal Analyses coupled with Mass Spectrometry (TGA-DTA-MS) analyses were performed in air atmosphere on a sample of about 3 mg obtained after dehydration on a hot plate at 393 K of 7.5 µL of the Gd/Glycine mixture solution. These analyses were performed in a Setaram Setsys Evolution 16 apparatus coupled to a mass spectrometer Hiden QGA300 for gas analysis.

X-Ray Diffraction patterns were obtained by a Bruker D8 diffractometer equipped with a Lynxeye detector and using Cu Kα radiation (λ = 1.54184 Å). XRD patterns were recorded at room temperature in the $10° \leq 2\theta \leq 60°$ range with a time of analysis equal to 2'47'', and Debye-Scherrer calculation has been used to determine average crystallites size.

Nitrogen adsorption/desorption analysis (77 K) was carried out with a Micromeritics Tristar 3020 instrument. Before each measurement, samples were outgassed at 398 K for 24 hours. The specific surface area was calculated by using the classic BET equation (Brunauer, Emmett, Teller).

Scanning electron microscope (SEM) observations were directly conducted on powder samples without prior preparation, using a FEI Quanta 200 electronic microscope, equipped either with a Back-Scattered Electron

115   Detector, in high vacuum conditions with a low accelerating voltage equal to 2 kV. These conditions were chosen

116   in order to induce a beam deceleration effect that led to high resolution images.

117   Finally, the amount of carbon in the powder was evaluated by the means of a LECO CS230 analyser using the

118   complete combustion of the samples in a large excess of O_2. Added Fe powder was used to assist the combustion.

119   The IR detection of the CO_2 formed was used to detect the carbon content. In order to get quantitative values, a

120   blank and a series of standards (steel containing wt% of carbon) were analysed before the samples.

121

122

123 **Results**

124   1) **Comparison of SCS / thermal conversion of Gd(NO$_3$)$_3$**

125   The comparison of TGA curves (Fig. 1a) of Gd/Glycine dried gel ($\phi = 1$) and gadolinium nitrate shows a clear

126   difference in the evolution of the mass losses according to the temperature. Concurrently with these mass losses,

127   DTA analyses show a small endothermic peak at 673 K for the former and a broad exothermic peak at 483 K for

128   the latter. These results confirmed that the ignition has occurred by the SCS reaction of the Gd/Glycine dried gel

129   according to reaction R1 (Table 1). The TGA analysis of glycine presented in SI-2 is identical to that presented in

130   [19].
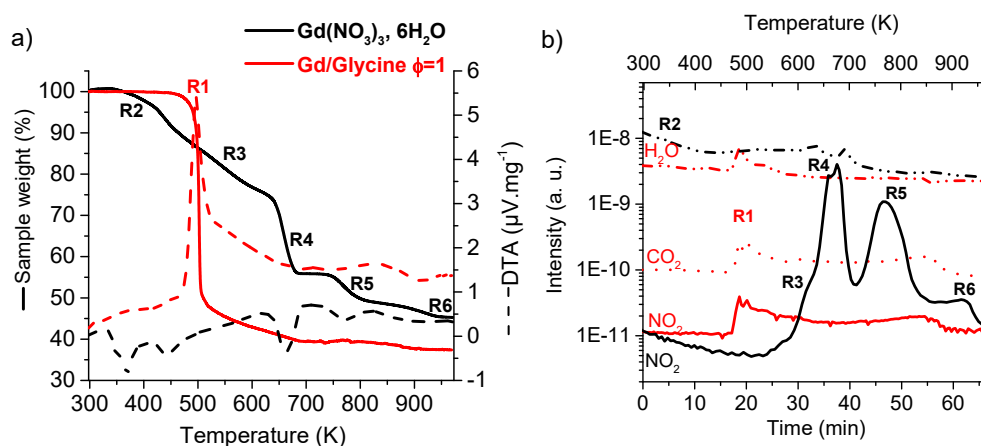
131

132 **Fig. 1.** a) TGA, DTA, and b) MS curves of gadolinium nitrate, $\phi = 1$ Gd/Glycine gel during a thermal treatment

133 (air atmosphere, heating rate 10 K.min^{-1})

134

135 **Table 1**

136 Equations and mass losses associated to thermal events observed during the TG analyses of Gd/Glycine ($\phi = 1$)

137 dried gel and of gadolinium nitrate hexahydrate. m_i and m_f : mass before and after the reaction. The thermal

138 treatment was done in air under a heating rate of 10 K / min. (*) Reactions described in reference [20]

139

Reaction		Theoretical m_f/m_i (%)	Experimental m_f/m_i (%)	Temperature onset (K)
$Gd(NO_3)_3, 6H_2O + \frac{5}{3}\phi\, NH_2CH_2CO_2H + \left(\frac{15}{4}(\phi - 1)\right) O_2$ $\rightarrow \frac{1}{2}\, Gd_2O_3 + \frac{10}{3}\phi\, CO_2 + (\frac{25}{6} + 6)\phi\, H_2O + \left(\frac{5}{6}\phi + \frac{3}{2}\right) N_2$	R1	37.5 (for $\phi = 1$)	38 (for $\phi = 1$)	483
$4(Gd(NO_3)_3, 6H_2O) \rightarrow Gd_4(NO_3)_{12}, 4H_2O + 20H_2O$	R2(*)	80	83	323

$Gd_4(NO_3)_{12}, 4H_2O \rightarrow Gd_4O(NO_3)_{10}, 4H_2O + N_2O_5$	R3(*)	92.5	87	513
$Gd_4O(NO_3)_{10}, 4H_2O \rightarrow Gd_4O_4(NO_3)_4, H_2O + 3N_2O_5 + 3H_2O$	R4(*)	71.7	74	626
$Gd_4O_4(NO_3)_4, H_2O \rightarrow Gd_4O_5(NO_3)_2 + N_2O_5 + H_2O$	R5(*)	86.8	87	738
$Gd_4O_5(NO_3)_2 \rightarrow 2Gd_2O_3 + N_2O_5$	R6(*)	87	93	850

More precisely, TGA curve of the gel (Gd/Glycine) displayed a mass loss of ~4% between 298 and 483 K caused by evaporation of water, a quick mass loss of ~ 52% at 483 K was caused by the ignition of the gel, and a total mass loss of ~ 62% at 973 K, is in agreement to theoretical mass loss 62.5% which is calculated on the basis of the SCS reaction of the dried gel (Table 1). At the end of ignition step, a white powder was formed, and regular decrease of mass of the SCS product was observed beyond 573 K, which was due to an elimination of organic residues as attested by carbon analyse showing a decrease of the carbon content from 0.5 wt% to 0.01 wt% respectively for powders heated at 573 K and 973 K.

The thermal decomposition of gadolinium nitrate hexahydrate reported by Melnikov [20] in nitrogen atmosphere, presents 5 endothermic steps (from R2 to R6). Although the TGA analyses were carried out under different atmospheres, the results are agreed with the report (Fig. 1a). All mass losses and peaks were assigned to the formation of oxynitrate as described in table 1.

MS curves (Fig. 1b) confirm the release of CO_2 and H_2O, during the ignition step of the SCS reaction, in agreement with reaction R1. N_2 is used as gas vector during the analysis that is why it cannot be detected as a product of the reaction R1. In addition, the release of NO_2 gas corresponds to a secondary reaction. This gas is also detected during the thermal decomposition of gadolinium nitrate hexahydrate in agreement with the reactions R3, R4, R5, R6.

Final products obtained after the TGA-DTA analyses were analysed by XRD (SI-3). XRD patterns show the formation of a cubic gadolinium oxide after a thermal treatment up to 973 K of gadolinium nitrate alone, whereas the products of the SCS reaction from synthesis in tubular furnace is a monoclinic gadolinium oxide obtained at 483 K (SI-2). This difference, which is a consequence of the temperature increase during the SCS reaction, will be discussed in the next part of this article.

2) Effect of processing parameters on the characteristics of the final products

As said previously, the SCS reaction was performed in a furnace leading to a volume combustion mode for the reactants. This mode of heating allows a precise control of the temperature ramp. Syntheses were done with Gd/Glycine ($\phi = 1$) mixtures with different ramp and XRD analyses of the final products were performed according to this parameter (Fig. 2). The results show that the crystalline compound Gd_2O_3 monoclinic was obtained for a heating rate higher than 3 K.min^{-1}, in these conditions, the final product is a white powder and ignition phenomenon were observed. On the contrary, tests carried out at lower heating rate did not lead to the ignition phenomenon. So the colour of the obtained powder is brown, associated to the high carbon content of these samples (> 4.7%). At heating rate of 3 K.min^{-1}, the powder was heterogeneous, the upper part of the sample was white, and the bottom was brown, which can mean a suffocation of the reaction at the bottom. For $\phi = 1$, the ratio C/Gd in the precursor is equal to 3.3 (see R1), depending on the processing conditions this ratio change from 0.08 to a value higher than 2 in the final product. The highest values were obtained when the ignition did not take place.
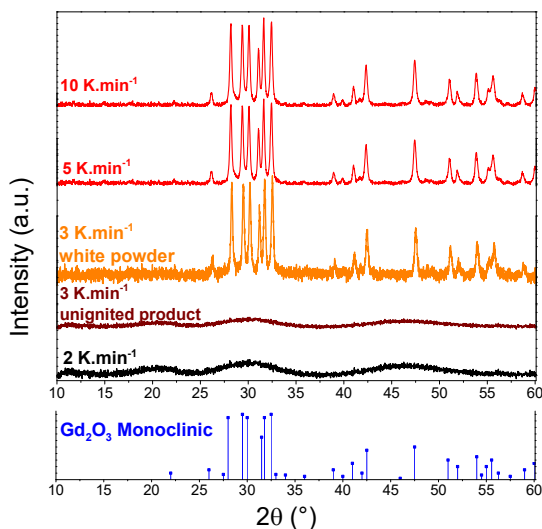
Fig. 2. XRD patterns of SCS reactions applied to Gd/Glycine $\phi = 1$ mixture with different heating rates (Gd_2O_3 monoclinic JCPDS 043-1015 (C))

Based on these results, a heating rate of 10 K.min^{-1} was selected for the elaboration of the following samples (Table 2).

In order to have a better understanding of the effect of glycine on the SCS reaction, we have undertaken several tests with various amounts of glycine ($0.3 < \phi < 2.2$). Several authors studied the effect of fuel/nitrate molar ratio on the final material, and their results provided a strong basis for the next studies [9, 21-29]. By comparing these studies, it clearly shows an effect of fuel richness on the morphology of the material and chemical composition, which changes with the mixture and the process (SI-1).

XRD patterns on the final products give several information's (SI4). The first one was the loss of crystallinity of the oxide when ignition does not occur, for low heating rate (< 3 K.min^{-1}) and with the lowest and the highest richness. The final products have a black colour, and a relatively high amount of carbon, meaning a low rate of transformation. The second observation relates to the phase transition observed according to the value of the richness in between 0.8 and 1.2. For $0.8 < \phi < 1.2$, monoclinic Gd_2O_3 was formed and cubic structure for the higher value of the richness. Not only the phase obtained, but also the morphology (specific area, crystallites size...) was affected by the change in the processing parameters (Table 2). For $\phi = 1$, the specific surface area increases with respect to the heating rate, and it is inversely proportional to the carbon content which can be likened to the efficiency of the SCS reaction. The high heating rate at 10 K.min^{-1}, is the best condition for the conversion, the specific surface area increasing slowly according to the richness in the range of $0.8 < \phi < 2.2$. As said previously, for the lowest richness ($\phi = 0.5$) the obtained amorphous powder has a quite high specific surface area which could be the result of the incomplete thermal decomposition of the mixture glycine/gadolinium nitrate. The increase of the richness leads also to an increase in the amount of carbon in the final products, which ultimately has the effect of reducing the size of the crystallites. However, the calculated surface area representative of the surface of the crystallites is higher than the measured one that can be explained by the embedment of the nanoparticles in a carbon matrix. This is revealed through the SEM observations, which clearly shows a porous structure for the sample obtained in the best conditions of reactivity ($\phi = 1$, heating rate = 10 K.min^{-1}). During ignition, the

203 decomposition reaction of reagents caused a large emission of gaseous species, which causes the formation of this
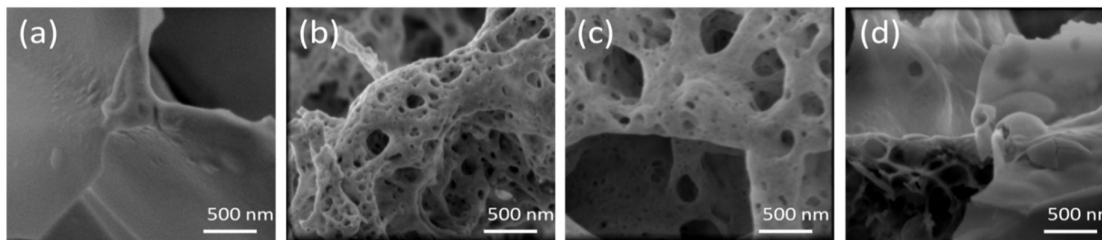204 porous structure (Figure 3).
205
206 **Table 2.**
207 Characteristics of final products obtained after SCS reaction of Gd/Glycine. The calculated surface area S (m².g⁻¹)
208 is obtained by the classical formulae $S = 3/d*\rho$ (d(nm) calculated by Debye-Scherrer formulae, ρ density of Gd_2O_3
209 = 7.41 g.cm⁻³). The error bars are about 1% for carbon content, 10% for crystallites size and 1% for the surface
210 area. Phases : amorphous (am.), Monoclinic (mon.), Cubic (cub.)

Fuel richness ϕ	Heating rate (K.min⁻¹)	Structure	Carbon (wt%)	C/Gd (at./at.)	Average crystallites size (nm)	Calculated specific area (m².g⁻¹)	Measured specific area (m².g⁻¹)
0.3		am.	2.6	0,4	-	-	27.2
0.5	10	am.	1.8	0,27	-	-	25.3
0.8		mon., cub.	0.7	0,1	28.6	14.2	10.3
1.0	1		8.8	1,4	-	-	0.3
	2	am.	7.8	1,27	-	-	0.5
	3		4.7	0,74	-	-	0.5
	3		0.5	0,08	29.3	13.7	2.0
	5	mon.	0.5	0,08	29.5	13.7	8.8
	10		0.5	0,08	29.5	13.7	9.8
1.2		mon., cub.	1.4	0,21	22.3	18.1	12.1
1.5		cub.	1.8	0,27	12.4	32.7	14.6
1.7	10	cub.	2.0	0,31	8.0	50.4	15.0
2.0		am.	11.2	1,9	-	-	16.1
2.2		am.	12.1	2,1	-	-	18.1

211

212

213   **Fig. 3.** SEM images of final products obtained after SCS reaction of Gd/Glycine mixtures a) 2 K.min^{-1} – ϕ = 1,

214   b) 10 K.min^{-1} – ϕ = 1, c) 10 K.min^{-1} – ϕ = 1.5, d) 10 K.min^{-1} – ϕ = 2

215

216   On the contrary, SEM images of the amorphous product (Fig. 3a) shows the formation of a coarse structure led to

217   the low specific area. An amorphous compound was also obtained for ϕ = 2 (Fig. 3d), but in this case, the high

218   value for a specific area could be caused by the release of gas arising from the incomplete conversion, i.e.

219   suffocation of the SCS reaction.

220

221

Discussion

1) Complexation

224   Glycine is used as a fuel for the SCS reaction, but can also be considered as a complexing agent for gadolinium

225   nitrate in particular because of amino and carboxyl functional groups in its structure. To understand these

226   interactions, comparative IR spectroscopy analyses were performed on glycine and Gd/Glycine gel at ϕ = 1 (Fig.

227   4).

228
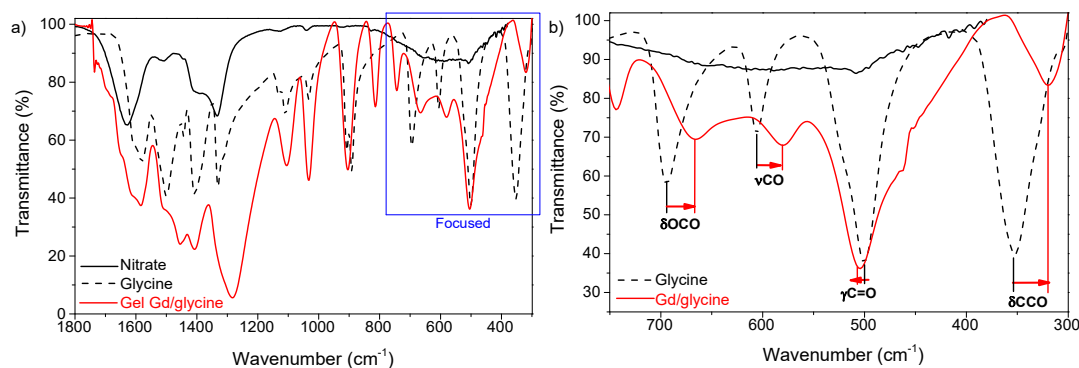
230   **Fig. 4.** IR spectra of the gel Gd/Glycine (ϕ = 1) compared to the glycine alone and the gadolinium nitrate

231   hexahydrate in the wavenumber range a) 1800-300 cm^{-1} and b) 750-300 cm^{-1} [26, 30-31]

232

233   It is difficult to obtain information from the domain of organic vibration bond between 1800 and 1000 cm^{-1} because

234   of simultaneous detection of nitrates and fuel bonds. The missing of organic vibrating bonds modification suggests

235   there was no chemical transformation of the reagents during gel formation step.

236   Information about interactions between gadolinium and glycine has been obtained by observing the shift of the

237   carboxylate function peaks between 750 and 300 cm^{-1}. This shift in the characteristic band associated with the

238   stretching of carboxylate is due to the strong interactions between the carboxylates and gadolinium. This

239   interaction was caused by a complexation of gadolinium ions with glycine during the formation of the gel. The

240   interaction between Gadolinium and Glycine is possible in with the mesomeric form of Glycine, which is a dipolar

241   molecule with a complexing carboxylate function. This complexation is very important for the combustion redox

242   reaction between the fuel and the nitrates. Indeed, results obtained during TG and MS analyses (Fig. 1, and SI-2)

show a transition from two endothermic thermal decompositions of reagents alone to one exothermic simultaneous decomposition of nitrates and glycine during the ignition.

2) Swelling effect and ignition

Only a few studies [22-23] report a swelling during the heat treatment of the gel obtained after mixing the nitrate with fuels (glycine, urea…). This phenomenon was not well studied, but it seems to have an impact on the ignition step as shown in Figure 5. It can be observed that the ignition was inhibited for the precursor, that has the highest swelling (Gd/Glycine ϕ=2).
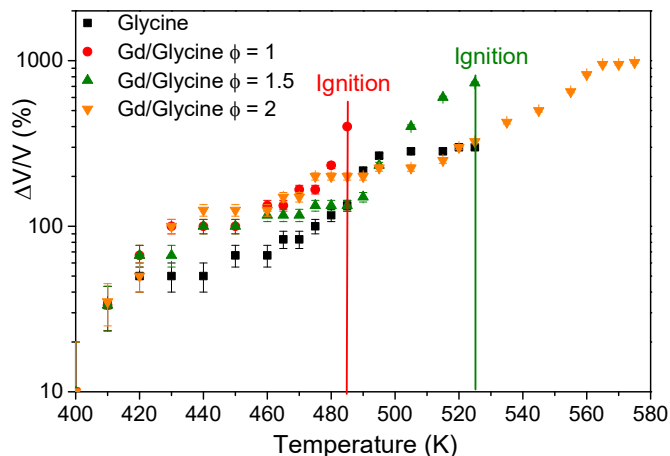

Fig. 5. Effect of the richness on the thermal swelling of the precursors (heating rate 10 K.min^{-1})

For a temperature of 483K, the volume of glycine alone increases more than twice, which is the same order of magnitude as the swelling of the precursors Gd/Glycine. This means that glycine has an important role in this process. This swelling is a consequence of the high viscosity of the gel and the generation of gases due to thermal decomposition. It is feasible that the viscosity of the gel with respect to glycine alone, is increased due to the interaction between the chemical groups of glycine and nitrates (see Fig. 4). However, two regimes can be highlighted: one corresponding to the thermal decomposition of a gel having a richness close to 1, i.e. in these conditions the final product obtained is a crystalline oxide, and the other corresponding to a higher richness (> 2) leading to an amorphous oxide (table 2).
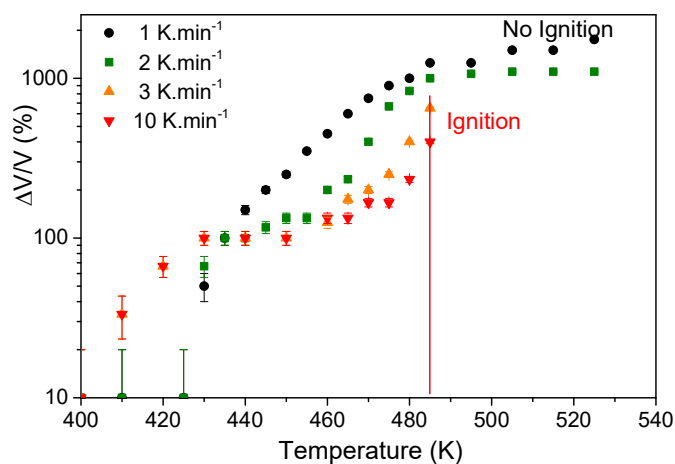
Fig. 6. Swelling of the precursors during the heat treatment: Effect of the heating rates Gd/glycine ($\phi = 1$)

In the first case (richness close to 1), the heating rate has an effect on the ignition phenomenom. For a heating rate lower than 3 K.min^{-1} the ignition was not observed (Fig. 6). This effect can be a consequence of the too low density of matter in the system induced by the higher volume increase. In these conditions, even if ignition can occur at a local scale, the reaction can not be self-propagated. At the transition-heating rate of 3 K.min^{-1}, two products were obtained, an amorphous brown powder with high carbon content (0.74%) on the bottom of the sample and a crystalline white powder with lower carbon content (0.08%) on the top (see table 2).The heterogeneity observed in this sample is probably due to the release of gaseous products by reaction R1. These gases rise from the bottom to the top of the mixture, and influenced the swelling and the reactivity of the system. For higher heating rates (> 3 K.min^{-1}), the SCS reaction occurs easily, because the density of matter is high enough to generate self-propagation of the reaction.

In the last case ($\phi > 2$), not only the swelling of glycine but also the penetration of oxygen is limiting factor for the reactivity. Indeed, under these conditions according to R1, oxygen is necessary for this reaction. The large volume of gas released by the reaction when the ignition occurs (500 liters / mol Gd for $\phi = 1$ to 500K) limits the ingress of oxygen and the progress of the reaction as indicated by the high carbon content measured in the final products (~2%wt.).

To conclude, the density of matter or more precisely the density of the chemical complex is a key parameter for the reactivity of the SCS reaction and for the ignition phenomena. In the case of an excess of glycine ($\phi > 2$), the access of oxygen could be another parameter that explains the lack of reaction (Fig. 2, Table 2).

3) Phase transformation

Powders obtained from the SCS reaction of different Gd/Glycine mixtures shows a transition phenomenon of gadolinium oxide crystalline structure formation when the fuel richness increases. The effect of fuel richness on SCS reaction can be explained through the estimation of the temperature attained during ignition. This temperature can be measured experimentally or calculated by thermodynamic considerations. In the former case, the temperature (T_c) is generally called "flame temperature" or "combustion temperature". Several reports [32-33] described that an increase of T_c with richness up to a value in the range of $1 < \phi < 1.5$ and after, a decrease of this

293   parameter for higher values of ϕ. In the latter case, the adiabatic temperature (T_{ad}) can be calculated using a simple

294   thermodynamic approach. T_{ad} increases substantially with the richness [34-35]. However, in a general point of

295   view, T_c is lower than T_{ad}. Several factors have been invoked to explain this difference: the experimental conditions

296   are not purely adiabatic [19], the fuel does not completely reacts with oxygen especially for fuel-rich conditions

297   [19, 33] and a part of heat produced by the ignition is dissipated by the considerable amount of gas generated. As

298   said previously, T_c decreases for high values of ϕ, which is the opposite trend compared to T_{ad}. This difference can

299   be caused by the utilization of an incorrect reaction route, which can change the energy balance of the process and

300   finely the calculation of T_{ad}. Only one report elucidated [9] the decrease of T_{ad} for $\phi > 1$, in the system of iron-

301   nitrate-glycine, certainly because of the set of the thermodynamic data used is representative of the SCS reaction.

302   To conclude, it is not so easy to obtain the value of the temperature reached during the ignition, especially when

303   $\phi \neq 1$. In this study, for stoichiometric conditions ($\phi = 1$), a low amount of residual carbon was measured in the

304   final products obtained by the SCS reaction R1 (Table 2), indicating that the reaction route proposed in Table 1 is

305   consistent. This result allows us to use a basic calculation to estimate T_{ad} as follow:

307   $$T_{ad} = T_0 - Q/\overline{c_p} \tag{1}$$

309   $$Q = \sum_j n_j \Delta_f H_j^0 - \sum_i n_i \Delta_f H_i^0 \tag{2}$$

311   $$\overline{c_p} = \sum_j n_j c_j \tag{3}$$

313   Where Q is the heat release during the reaction and, $\overline{c_p}$ the average specific heat capacity of the products at room

314   temperature. T_o is the ambient temperature, i and j respectively specify reactants and products and n_i and n_j are the

315   amounts of each compound. The ΔH_f^0 and c_j values of the compounds are presented Table 3.

316   **Table 3.**

317   Standard enthalpies of formation and heat capacities for Gadolinium nitrate hexahydrate – Glycine system from
318   [19, 36]

Compounds	ΔH_f^0 (kJ.mol^{-1})	c_p (J.mol^{-1}.K^{-1})
Gd(NO$_3$)$_3$, 6H$_2$O	-3072.3	
Glycine, solid	-528.5	
Gd$_2$O$_3$, solid	-1825	106.7
H$_2$O (g)	-241.8	30
CO$_2$ (g)	-393.1	43
N$_2$ (g)	0	27
O$_2$ (g)	0	25

321   The adiabatic temperature calculated (T_{ad}) for $\phi = 1$ is close to 1600 K, which is higher than the temperature of

322   1473 K proposed in reference [37] for the transition cubic/monoclinic of gadolinium oxide. The monoclinic

323 structure of the gadolinium oxide powders synthesise in this study is in agreement with this result (Table 2). As

324 discussed previously for $\phi \neq 1$, a decrease of the temperature reached by the SCS reaction was observed, that can

325 explain the formation of the cubic gadolinium oxide structure obtained under the same combustion temperatures

326 for fuel-lean or fuel-rich (ϕ = 0.8 and $1.5 < \phi < 1.7$). However, the thermodynamic calculation is not able to

327 predict the lack of ignition and the formation of amorphous final products, for large excess of one of the reagents

328 ($\phi < 0.5$ or $\phi > 2$). In these conditions, the reagent acts as a diluting compound for the SCS reaction and was

329 associated with a diluting effect and its endothermic decomposition induces an inhibition for ignition.

330 The lack of ignition with $\phi = 0.5$ and $\phi = 2$ Gd / Glycine mixtures and the optimal ignition of Gd / Glycine

331 stoichiometric richness mixtures were confirmed by IR analyses on the final powders (Fig. 7).
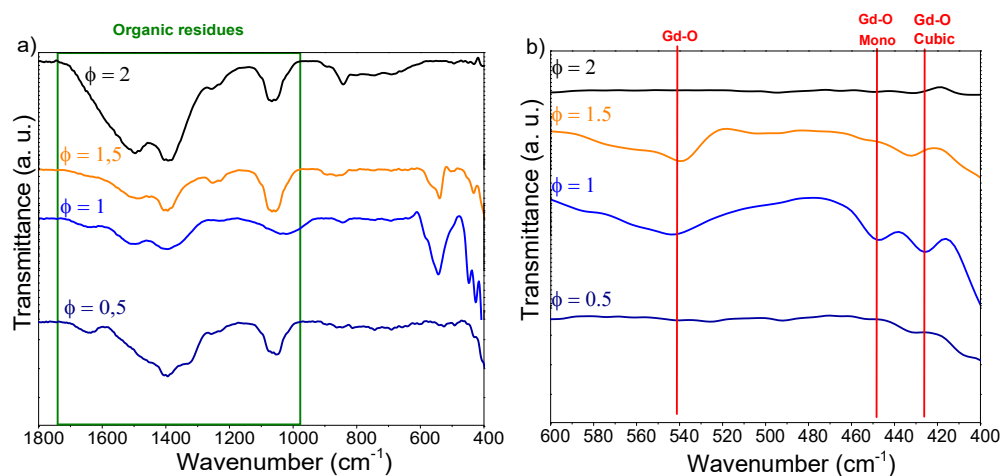
332

333 **Fig. 7.** IR spectra of SCS reaction final products obtained with Gd/Glycine mixtures with different ϕ, in the

334 wavenumber range a) 1800 - 400 cm^{-1} and b) zoom in the area 600 - 400 cm^{-1} (air atmosphere, heating rate 10

335 K.min^{-1})

336

337 IR spectra of the compound obtained without ignition ($\phi = 0.5$, $\phi = 2$, Fig. 7) show a lack of gadolinium-oxygen

338 bonds between 700 and 400 cm^{-1}, and the main presence of organic compounds between 1800 and 1000 cm^{-1}.

339 These organic bonds are also present in the IR spectra of the final products, but gadolinium-oxygen bonds were

340 detected too. Furthermore, organic residues are fewer presents in IR spectra of final powders obtained with

341 stoichiometric richness mixtures, which was confirmed by carbon content measures (Table 2). IR spectra of

342 powders are similar than their XRD patterns (SI-4) and confirm the formation of crystalline nanoparticles after

343 ignition and of organic residues at $\phi = 0.5$ and $\phi = 2$. In the case of $\phi = 0.5$ and $\phi = 2$ Gd/Glycine mixtures, a

344 thermal treatment at 973 K is necessary to obtain the final cubic gadolinium oxide.

345

346

Conclusion

348 The conversion of gadolinium nitrate into oxide was obtained by SCS reaction with glycine as fuel at temperature

349 about 723 K lower than the classical thermal denitration temperature. For a stoichiometric ratio of glycine /

350 gadolinium nitrate ($\phi = 1$), monoclinic Gd$_2$O$_3$ powder are obtained with a specific surface area of about 10 m^2.g^{-1},

a small amount of residual carbon and good crystallinity. The ignition of the precursors leading to the conversion nitrate / oxide, was observed at a temperature of about 483 K.

The implementation of this reaction with glycine causes significant swelling of the precursors during the temperature increase up to the ignition. This swelling is related to the decomposition of glycine. Several experimental parameters: the heating rate, the richness influence the amplitude of this phenomena. When the swelling is too high (rate of heating rate < 3 K.min^{-1}, richness $\phi > 2$), the ignition is not observed and an amorphous compound is obtained. These results indicate that the density of matter before the ignition is a key parameter for the reaction that modifies the reactivity of the system and induces structural changes. For intermediate richness ($\phi = 0.8$, 1.5, 1.7), the end-products have a cubic structure, which is the stable structure of this oxide at low temperature, or a mixture of monoclinic and cubic Gd_2O_3. Adiabatic temperature calculations of the reaction are consistent with the crystalline phases observed.

These findings of actinide surrogates suggest that, the new route will be a promising path for the recycling of actinides of the Generation IV reactors systems. However, the high swelling of the glycine would be a drawback for the application of such fuel in an industrial process, notably for the conversion of actinides. Works are in progress to evaluate other fuels such as citric acid, β-alanine.

Acknowledgements

References

[1] The full report (2002) A technology roadmap for generation IV nuclear energy systems, GIF-002-00. http://www.gen-4.org. Accessed 10 Sept 2018

[2] OECD/NEA (2014) GEN IV International Forum. Technology roadmap update for generation IV nuclear energy systems

[3] A. G. Merzhanov, Self-propagating high-temperature synthesis of refractory compounds, *Vestn. Akad. Nauk-SSSR* 10, (1976) p.76-84

[4] A. G. Merzhanov, SHS-process: combustion theory and practice, *Arch. Combust.* 191, N 1/2, (1981) p.23-48.

[5] K. C. Patil, Advanced ceramics: Combustion synthesis and properties, *Bull. Mater. Sci.* 16 (1993) 533-541.

[6] K. C. Patil, K. Suresh, A combustion process for the instant synthesis of γ-iron oxide, *J. Mater. Sci. Lett.* 12 (1993) 572-574.

[7] K. C. Patil, S. T. Aruna, T. Mimani, Combustion synthesis: an update, *Curr. Opin. Solid State Mater. Sci.* 6(6), (2002) 507-512

[8] K.V. Manukyan, Solution Combustion Synthesis of Nano-Crystalline Metallic Materials: Mechanistic Studies, *J. Phys. Chem. C* 117, (2013) 24417−24427

390   [9] A. S. Mukasyan, P. Epstein, P. Dinka, Solution combustion synthesis of nanomaterials, *Proc. Combust.*
391   *Inst.* 31 (2007) 1789-1795

392   [10] D. Sanjay Kumar, K. Ananthasivan, R. Venkata Krishnan, S. Amirthapandian, A. Dasgupta, Bulk
393   synthesis of nanocrystalline urania powders by citrate gel-combustion method, *J. Nucl. Mater.* 468
394   (2016) 178-193

395   [11] D. Sanjay Kumar, K. Ananthasivan, R. Venkata Krishnan, S. Amirthapandian, A. Dasgupta, Studies on
396   the synthesis of nanocrystalline Y_2O_3 and ThO_2 through volume combustion and their sintering, *J. Nucl.*
397   *Mater.* 479 (2016) 585-592

398   [12] D. Sanjay Kumar, K. Ananthasivan, R. Venkata Krishnan, D. Maji, A. Dasgupta, A novel gel
399   combustion procedure for the preparation of foam and porous pellets of UO_2, *J. Nucl. Mater.* 483
400   (2017) 199-204

401   [13] D. Sanjay Kumar, K. Ananthasivan, R. Venkata Krishnan, A. Senapati, reaction mechanism and kinetic
402   analysis of citrate gel-combustion synthesis of nanocrystalline Urania, *J. Nucl. Mater.* 131 (2018)
403   2467–2476

404   [14] S. Anthonysamy, K. Ananthasivan, V. Chandramouli, I. Kaliappan, P.R.V. Rao, Combustion synthesis
405   of urania-thoria solid solutions, *J. Nucl. Mater.* 278(2-3) (2000) 346-357

406   [15] Y.P. Naik, G.A. Ramarao, A. Banthiya, D. Chaudhary, C. Arora, Synthesis and characterization of
407   nano-structured $Th_{1-x}Ce_xO_2$ mixed oxide, *J. Therm. Anal. Calorim.* 107 (2012) 105-110

408   [16] G. Peter-Soldani, Approche structurale et phénoménologique de la conversion directe ou modifiée de
409   nitrates d'actinide(s) en oxyde, PhD Thesis, University LILLE 1 (2013)

410   [17] G. Peter-Soldani, S. Grandjean, F. Abraham, Process for preparing a powder comprising a solid
411   solution of uranium dioxide and of a dioxide of at least one other actinide and/or lanthanide element,
412   Patent WO2015059188A1 (2015)

413   [18] A. Varma, A.S. Mukasyan, Combustion synthesis of advanced materials: Fundamentals and
414   applications, *Korean J. Chem. Eng.* 21(2) (2004) 527-536.

415   [19] A. Varma, A.S. Mukasyan, A.S. Rogachev, K.V. Manukyan, Solution Combustion Synthesis of
416   Nanoscale Materials, *Chem. Rev.* 116 (23) (2016) 14493-14586

417   [20] P. P. Melnikov, V. A. Nascimento, L. Z. Zanoni Consolo, Computerized modeling of intermediate
418   compounds formed during thermal decomposition of gadolinium nitrate hydrate, *Russ. J. Phys. Chem.*
419   (2012) p.1781-1785

420   [21] P. Bera, S. T. Aruna, K. C. Patil, M. S. Hedge, Studies on Cu/CeO2: A New NO Reduction Catalyst, *J.*
421   *Catal.* 186 (1999) 36-44

422   [22] K. Deshpande, A. Mukasyan, A. Varma, Direct synthesis of iron oxide nanopowders by the combustion
423   approach: Reaction mechanism and properties, *Chem. Mater.* 16(24) (2004) 4896-4904.

424   [23] K.C. Patil, M.S. Hegde, T. Rattan, S.T. Aruna, Chemistry of nanocristalline oxides materials,
425   Combustion synthesis, properties and applications, World scientific : Singapore (2008).

426   [24] S.R. Nair, R.D. Purohit, A.K. Tyagi, P.K. Sinha, B.P. Sharma, Role of glycine-to-nitrate ratio in
427   influencing the powder characteristics of La(Ca)CrO3, *Mater. Res. Bull.* 43(6) (2008) 1573-1582.

428   [25] L. Yulin, Y. Jun, L. Xiaoci, H. Weiya, T. Yu, Z. Yuanming, Combustion synthesis and stability of
429   nanocrystalline La_2O_3 via ethanolamine-nitrate process, *J. Rare Earths* 30(1) (2012) 48-52.

430   [26] Q. G. Wang, R.R. Peng, C.R. Xia, W. Zhu, H.T. Wang, Characteristics of YSZ synthesized with a
431   glycine-nitrate process, Ce*ram. Int.* 34(7) (2008) 1773-1778.
432   [27] C. H. Jung, S. Jalota, S.B. Bhaduri, Quantitative effects of fuel on the synthesis of Ni/NiO particles
433   using a microwave-induced solution combustion synthesis in air atmosphere, *Mater. Lett.* 59(19-20)
434   (2005) 2426-2432.
435   [28] M. Valefi, C. Falamaki, T. Ebadzadeh, M.S. Hashjin, New insights of the glycine-nitrate process for the
436   synthesis of nano-crystalline 8YSZ, *J. Amer. Ceram. Soc.* 90(7) (2007) 2008-2014
437   [29] P. Erri, J. Nader, A. Varma, Controlling combustion wave propagation for transition metal/alloy/cermet
438   foam synthesis, *Adv. Mater.* 20(7) (2008) 1243.
439   [30] A. Gomez-Zavagliaab, R. Fausto, Low-temperature solid-state FTIR study of glycine, sarcosine and
440   N,N-dimethylglycine: observation of neutral forms of simple α-amino acids in the solid state, *Phys.*
441   *Chem. Chem. Phys.* 5 (2003) 3154-3161
442   [31] G. Fischer, X. Cao, N. Cox, M. Francis, The FT-IR spectra of glycine and glycylglycine zwitterions
443   isolated in alkali halide matrices, *Chem. Phys.* 313 (2005) 39-49
444   [32] L. A. Chick, L. R. Pederson, G. D. Maupin, J. L. Bates, L. E. Thomas, G. J. Exarhos, Glycine-nitrate
445   combustion synthesis of oxide ceramic powders, *Mater. Lett.* 10 (1990) 6.
446   [33] C. C. Hwang, T. Y. Wu, Synthesis and characterization of nanocrystalline ZnO powders by a novel
447   combustion synthesis method, *Materials Science and Engineering B 111* (2004) 197–206
448   [34] R.D. Purohit, B.P. Sharma, K.T. Pillai, A.K. Tyagi, Ultrafine ceria powders via glycine-nitrate
449   combustion, *Materials Research Bulletin* 36 (2001) 2711–2721
450   [35] K. Tahmasebi, M.H. Paydar, The effect of starch addition on solution combustion synthesis of
451   Al_2O_3–ZrO_2 nanocomposite powder using urea as fuel, *Materials Chemistry and Physics* 109 (2008)
452   156–163
453   [36] S-X. Xiao, A-T. Li, J-H. Jiang, S. Huang, X-Y. Xu, Q-G. Li, Thermochemical analyses on rare earth
454   complex of gadolinium with salicylic acid and 8-hydroxyquinoline, *Thermochimica Acta* 548 (2012)
455   33-37
456   [37] S. S. Hadke, M. T. Kalimila, S. Rathkanthiwar, R. Sonkusare, S. Gour, A. Ballal, Monoclinic to cubic
457   phase transformation in combustion synthesized gadolinium oxide, *Mater. Today Proceedings* 2 (2015)
458   1276-1281

Measure of the swelling of the Gel

- 1 K.min^{-1}
- 10 K.min^{-1}

XRD : 1 K.min^{-1} - Amorphous product

XRD : 10 K.min^{-1} - Gadolinium oxide